Phase Transition Approach to High Temperature Superconductivity

Universal Properties of Cuprate Superconductors

高温超导中的相变方法

T. Schneider & J. M. Singer

Imperial College Press
世界图书出版公司

Phase Transition Approach to High Temperature Superconductivity

Universal Properties of Cuprate Superconductors

T. Schneider & J. M. Singer
University of Zurich, Switzerland

世界图书出版公司

书　　名：Phase Transition Approach to High Temperature Superconductivity
作　　者：T.Schneider & J.M.Singer
中 译 名：高温超导中的相变方法
出 版 者：世界图书出版公司北京公司
印 刷 者：北京世图印刷厂
发　　行：世界图书出版公司北京公司 (北京朝内大街 137 号　100010)
联系电话：010-64015659, 64038347
电子信箱：kjsk@vip.sina.com
开　　本：24 开　　印　张：18.5
出版年代：2004 年 4 月
书　　号：7-5062-6620-2/O・473
版权登记：图字:01-2004-1609
定　　价：56.00 元

Published by

Imperial College Press
57 Shelton Street
Covent Garden
London WC2H 9HE

Distributed by

World Scientific Publishing Co. Pte. Ltd.
P O Box 128, Farrer Road, Singapore 912805
USA office: Suite 1B, 1060 Main Street, River Edge, NJ 07661
UK office: 57 Shelton Street, Covent Garden, London WC2H 9HE

British Library Cataloguing-in-Publication Data
A catalogue record for this book is available from the British Library.

PHASE TRANSITION APPROACH TO HIGH TEMPERATURE SUPERCONDUCTIVITY
Universal Properties of Cuprate Superconductors

ISBN 1-86094-241-5

Preface

The discovery of superconductvity at $30K$ by Bednorz and Müller in 1986 ignited an explosion of interest in high temperature superconductivity. The initial development rapidly evolved into an intense worldwide research effort that still persists after more than a decade to understand the phenomenon of cuprate superconductivity, to search for ways to raise the transition temperature and to produce materials which have the potential for technological applications. During the past decade of research on this subject significant prograss has been made on both the fundamental science and technological application fronts. A great number of experimental data is now available on the cuprates, and various properties have been well characterized using high quality single crystals and thin films. Despite this enormous research effort, the underlying mechanisms responsible for superconductivity in the cuprates are still open to question. Nevertheless, we believe that the overall picture of the experimental situation is clear enough to warrant the writing of a textbook that presents our understanding from the phase transition point of view, surveys and identifies thermal and quantum fluctuation effects, identifies material independent universal properties and provides constraints for the microscopic description of the various phenomena. The aim is to present this material in a format suitable for the use in a graduate level course.

A survey of phase transitions in cuprate superconductors, including the normal conductor to superconductor, normal conductor to insulator and superconductor to insulator transitions, tuned by a variation of temperature, doping, magnetic field, disorder etc., must be based on a background of theory of thermal and quantum critical phenomena, found in textbooks and review articles. Brief introductory chapters and appendices covering special topics provide a sketch of this background.

Topics discussed include:

- Experimental evidence for classical critical behavior: critical behavior close to optimum doping; specific heat, penetration depth, magnetization, crossing point phenomenon, magnetic torque, magnetic field tuned phase transitions, doping dependence of finite temperature critical properties, universal scaling functions, universal relation between specific heat, transition temperature, correlation length and penetration depths at criticality, finite size scaling, corrections to scaling, dimensional crossover, Kosterlitz-Thouless transitions in thin films.

- Evidence for quantum critical properties: superconductor to insulator transition in two dimensions; universal relation between transition temperature and zero temperature penetration depth; universal conductance at criticality; nature of the insulating phase.

- Implications: failure of the interlayer tunneling model, supression of the transition temperature due to dimensional crossover and quantum fluctuations, pseudogap features, doping and pressure dependence of critical amplitudes, Bose gas approach, effective pair mass and emerging phase diagrams.

The immense scope of this subject dictated a selective choice of the experimental data cited to illustrate the progress made in this field over the past decade. For comprehensive accounts of specific topics in high temperature superconductivity the reader is referred to various review articles.

Finally, we are pleased to acknowledge the assistance of many collegues in encouraging our efforts, in helping to guide the focus of several revisions, and on providing generous assistance in improving the quality of the presentation. We have benefited from discussions with (or encouragement by) J. Hofer, M. Willemin, H. Keller, K. A. Müller, C. Meingast, H. Beck, P. Martinoli, J. Perret, Ø. Fischer, J.-M. Triscone, G. Triscone, A. Junod, M. Roulin, C. Rossel, P. F. Meier, E. Stoll, I. Herbut, Z. Tesanovic, F. Nogueira, A. Sudbø, V. Loktev and J. Engelbrecht (we apologize in advance to all those inadvertently omitted). Moreover, we appreciate the support given by the Physics Department of the University of Zurich, the Swiss National Science Foundation and Imperial College Press, London.

Zurich, December 1999 *T. Schneider and J. M. Singer*

Contents

Chapter 1

Introduction

1.1 Cuprate superconductors

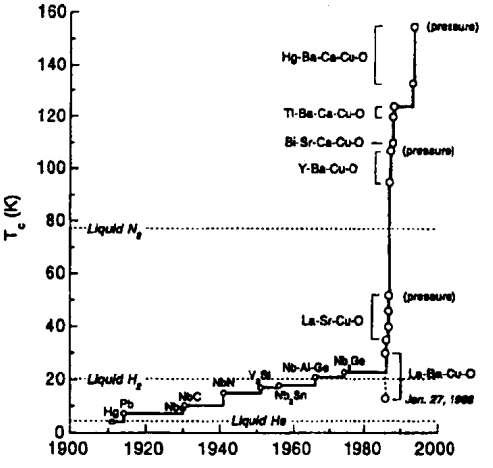

FIGURE 1.1: Maximum superconducting transition temperature T_c versus time. Taken from [189].

The dramatic increases in the transition temperature T_c that has been observed since 1986 are illustrated in Fig. 1.1 where the maximum value of T_c is plotted versus date. Prior to 1986, the A15 compound Nb_3Ge with $T_c \approx 23K$ held the record for the highest value of T_c [85]. After the discovery of superconductivity at 30K in the cuprate system La-Ba-Cu-O [24], the maximum value of T_c has increased steadily to its current maximum value in $HgBa_2Ca_2Cu_3O_8$

[260]. When this compound is subjected to pressure [43], the critical temperature T_c increases to 166K.

1.1.1 Structure

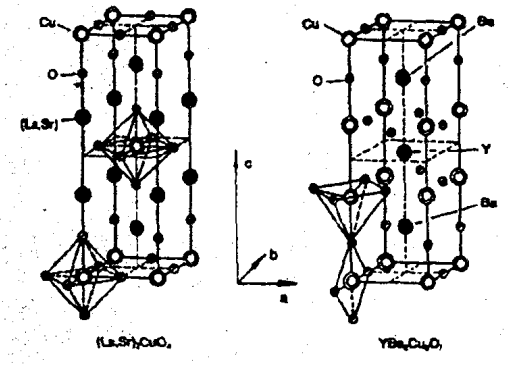

FIGURE 1.2: Schematic crystal structure of $La_{2-x}Sr_xCuO_4$ and $YBa_2Cu_3O_{7-x}$. Taken from [266].

Approximately 100 different cuprate materials, many of which are superconducting, have been discovered since 1986. These materials are layered perovskite-type structures which consist of CuO_2 planes separated by layers comprised of other elements A and oxygen, A_mO_n, and, in some cases, layers of Ln ions. The A_mO_n layers act as charge reservoirs and control the doping of the CuO_2 planes with charge carriers. The mobile charge carriers are believed to reside primarily within the CuO_2 planes. In several of the compounds containing Ln layers, the Ln ions with partially-filled $4f$ electron shells and magnetic moments have been found to order antiferomagnetically at low temperatures [190]. Fig. 1.2 shows the structure of two of the most extensively studied materials, $La_{2-x}Sr_xCuO_4$ and $YBa_2Cu_3O_{7-x}$. Their so-called *parent compounds* are La_2CuO_4 and $YBa_2Cu_3O_6$, refering to the undoped, antiferromagnetic, non-superconducting structure. The La_2CuO_4 layering scheme consists of equally spaced, CuO_2 sheets, with the oxygen atoms stacked one atop the other, the copper ions alternating between two sites in adjacent layers. Half of the oxygen are in the planes, and the other half between them. In La_2CuO_4 the unit cell contains two CuO_2 planes, with a spacing of ≈ 6Å. We see from Fig. 1.2 that in $YBa_2Cu_3O_7$ three planes containing Cu and O are sandwiched between two planes containing Ba and O and one plane containing Y. There are two CuO_2 planes that have the Y plane between them. A third

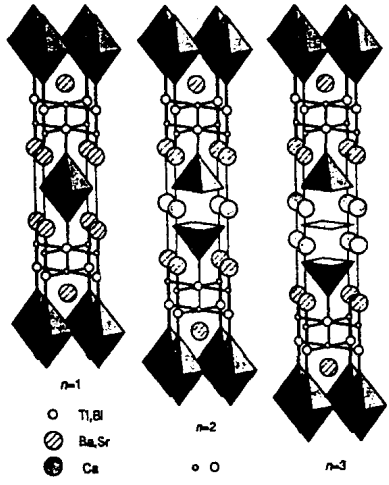

FIGURE 1.3: Multilayer materials: Structures of 2201, 2212 and 2223 $Bi-Sr-Ca-Cu-O$ (BSCCO) and $Tl-Ba-Ca-Cu-O$ (TBCCO) systems with $n = 1, 2, 3$ directly adjacent CuO_2-layers. Taken from [5].

CuO-plane, often referred to as chains, consists of $-Cu-O-Cu-O-$ chains along the b-axis. Thus, there are two CuO_2 planes per unit cell. Even three or more closely spaced CuO_2 planes are realized in some of the Bi, Tl and Hg based cuprates (see Fig. 1.3).

1.1.2 Doping

Metallic behavior is derived from the insulating and antiferromagnetic parent compounds by partial substitution of out-of-plane ions or by adding or removing oxygen. In $YBa_2Cu_3O_7$ hole doping is achieved by changing the oxygen content from $O_{6.5}$ to O_{7-x}, while La_2CuO_4 can be doped either by alkaline earth ions or oxygen to exhibit superconducting properties. The phase diagram of $La_{2-x}Sr_xCuO_4$ depicted in Fig. 1.4 shows that holes are very efficient in destroying the antiferromagnetic long-range ordered state. Indeed, for $x = 0$, $La_{2-x}Sr_xCuO_4$ is a highly anisotropic antiferromagnetic insulator ($T_N \approx 300K$). It is well described by a $2D$ $S = 1/2$ Heisenberg antiferromagnet. On adding Sr, T_N drops very sharply and vanishes at $x \approx 0.01$. Then, there is the spin glass phase, and magnetic short range order does persist up to fairly high doping levels, as elucidated by inelastic neutron scattering. Electrical resistivity measurements reveal, that at a certain doping level – the so

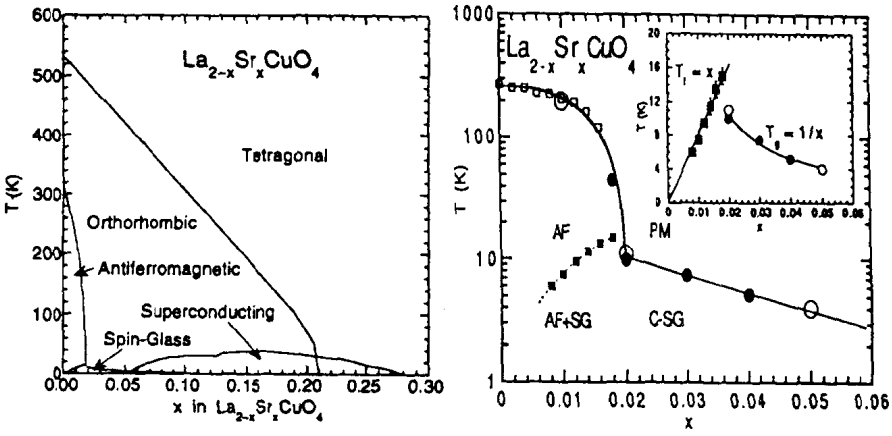

FIGURE 1.4: Left panel: structural, magnetic and superconducting phase diagram of $La_{2-x}Sr_xCuO_4$. Taken from [141]. Right panel: $La_{2-x}Sr_xCuO_4$ in the doping regime $x < 0.06$. Abbreviations: PM, paramagnetic; AF, antiferromagnetic; SG, spin-glass; CSG, cluster spin-glass; T_f and T_g, spin-glass freezing temperatures for $x < 0.02$ and $x > 0.02$, respectively. Taken from [142].

called underdoped limit x_u – the system undergoes at $T > 0$ an insulator to anomalous conductor transition and at $T = 0$ an insulator to superconductor transition [299]. In $La_{2-x}Sr_xCuO_4$ this occurs close to $x_u \approx 0.05$, where x is the hole concentration per Cu atom in the CuO_2 plane. Many inelastic neutron scattering measurements on the $La_{2-x}Sr_xCuO_4$ system have been carried out. They established that AF correlations survive into the normal conducting as well as the superconducting regime, which may be important with regard to the mechanism for high temperature superconductivity of the layered cuprates. As the hole concentration is increased, the superconducting transition temperature T_c rises, reaches a maximum value T_c^m at x_m. In the so called underdoped regime $x_u \leq x \leq x_m$ the material exhibits anomalous normal state properties. With further increase of x the compound becomes more metallic, but now T_c decreases and finally vanishes in the overdoped limit x_o. At x_o a superconductor to normal conductor transition is expected to occur at $T = 0$. Such a (T, x) phase diagram appears to be generic for cuprate superconductors. Examples include $La_{2-x}Sr_xCuO_4$, $YBa_2Cu_3O_{7-x}$, $Y_2Ba_4Cu_7O_{15+x}$ [87], $Bi_2Sr_2CuO_{6+x}$, $Bi_2Sr_2CaCu_2O_{8+x}$ [102], $Tl_2Ba_2CuO_{6+x}$ [223] and $HgBa_2CuO_{4+x}$ [82]. Experimental data for the doping dependence of the superconductor transition temperature are shown in Fig. 1.5.

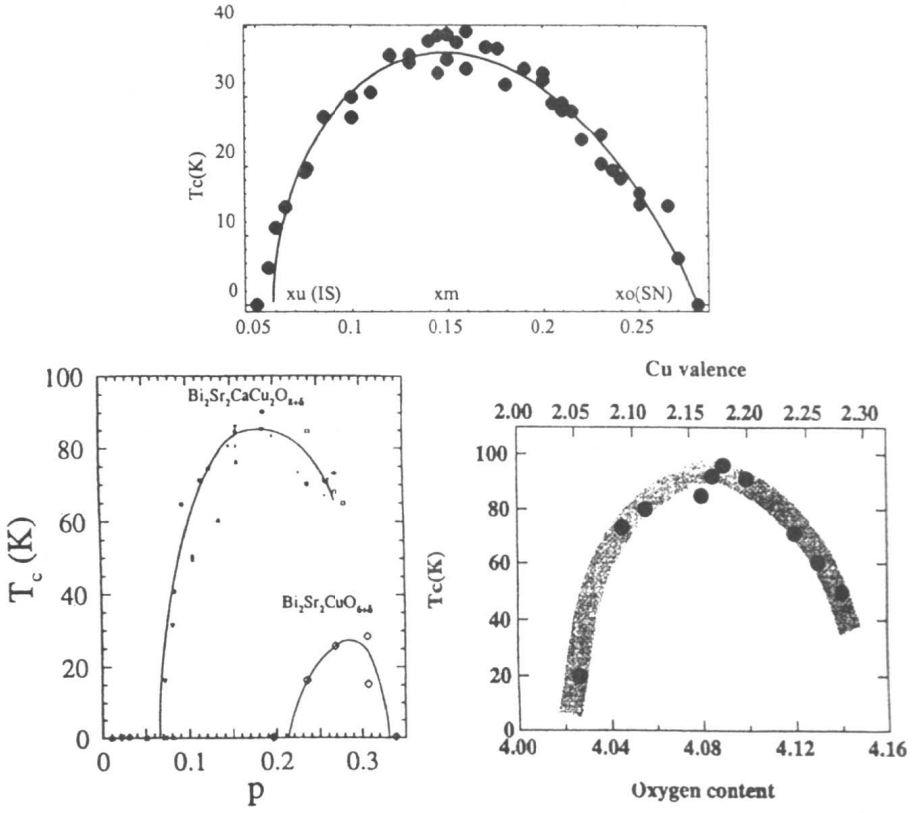

FIGURE 1.5: Upper Panel: Superconducting transition temperature T_c versus x for bulk $La_{2-x}Sr_xCuO_4$. Data taken from [299], [307], [208] and [83]. x_u and x_o denote the under- and overdoped limits, respectively, where T_c vanishes, while at x_m, corresponding to optimal doping, the transition temperature reaches its maximum value. Lower panel, left: T_c versus hole concentration p for $Bi_2Sr_2CuO_{6+p}$ and $Bi_2Sr_2CaCu_2O_{8+p}$, taken from [102]. Lower panel, right: T_c versus hole concentration δ for $HgBa_2CuO_x$, taken from [82].

Apparently, a unique property of cuprate superconductors is the occurrence of a phase transition line $T(x)$ in the temperature-doping plane, which separates the superconducting from the normal conducting phase. It should be recognized that this feature is absent in conventional superconductors. In $La_{2-x}Sr_xCuO_4$, $Bi_2Sr_2CuO_{6+x}$ and $HgBa_2CuO_{4+x}$ both, the underdoped and overdoped limits are experimentally accessible, while in other compounds, including $Bi_2Sr_2CaCu_2O_{8+x}$ and $YBa_2Cu_3O_{7-x}$, only the underdoped and optimally doped regimes appear to be accessible. Another prominent example is $Y_{1-x}Pr_xBa_2Cu_3O_{7-\delta}$, which becomes more and more underdoped as x-increases and T_c vanishes at $x \approx 0.55$.

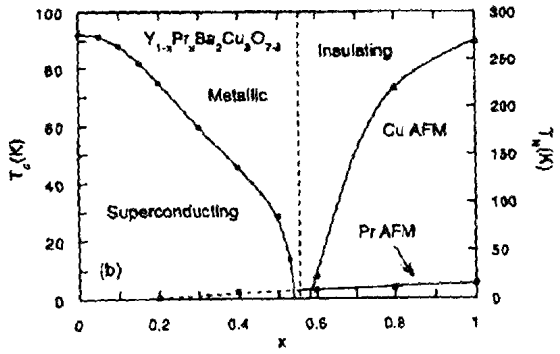

FIGURE 1.6: Phase diagram in the (T, x) - plane of $Y_{1-x}\,Pr_x\,Ba_2Cu_3O_{7-\delta}$, showing metallic, superconducting, insulating and antiferrromagnetically ordered regions. Taken from [214].

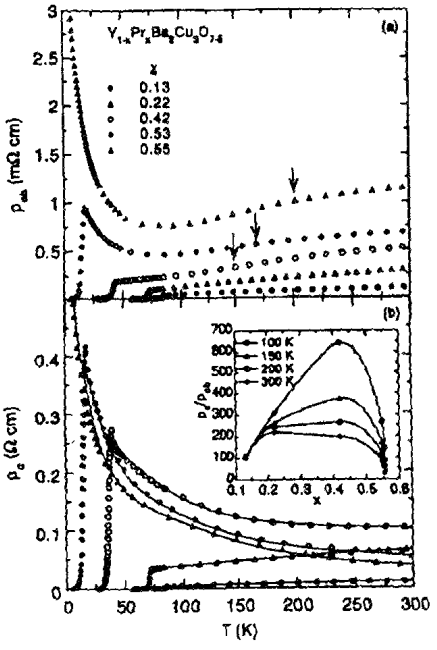

FIGURE 1.7: In-plane resistivity $\rho_{ab}(T)$ (a) and out-of-plane resistivity $\rho_c(T)$ (b) for a $Y_{1-x}\,Pr_x\,Ba2Cu3O_{7-\delta}$ single crystal. Inset to panel (b): anisotropy ρ_{ab}/ρ_c versus x at different temperatures. Taken from [139].

Displayed in Fig. 1.6 is the (T,x) phase diagram of this material. In any case, the occurrence of this phase transition line and the associated two critical endpoints, occurring in the underdoped and overdoped limits where T_c vanishes, leads to the important question, how the ground state of the cuprates evolves as a function of doping.

This evolution is reflected in the temperature dependence of the ab-plane and c-axis resistivities $\rho_{ab}(T)$ and $\rho_c(T)$ (see, e.g., [48]). Both $\rho_{ab}(T)$ and $\rho_c(T)$ exhibit in the underdoped region a crossover from metallic conducting (i.e., $d\rho/dT > 0$) to semiconducting behavior (i.e., $d\rho/dT < 0$) with decreasing temperature, $\rho_c(T)$ is semiconducting or metallic close to optimal doping, depending on the material, and $\rho_{ab}(T)$ and $\rho_c(T)$ are both metallic in the overdoped region. As an example of the evolution of $\rho_{ab}(T)$ and $\rho_c(T)$ with doping we refer to the data shown in Fig. 1.7 for a $Y_{1-x}Pr_xBa_2Cu_3O_{7-\delta}$ single crystal. It should be noted, however, that insulating features of $\rho_c(T)$ close to optimal doping are most likely due to incoherent tunneling [139]. The generic phase diagram of the cuprates as a function of dopant concentration appears to be a critical line $T_c(x)$. At the critical endpoints, corresponding to the underdoped ($x = x_u$) and overdoped ($x = x_o$) limits, T_c vanishes, so that at $T = 0$ and $x = x_u$ a doping tuned insulator to superconductor (IS) transition, and at $x = x_o$ a superconductor to normal metallic conductor (SN) transition occurs. Resistivity measurements in $60T$ pulsed magnetic fields to quench superconductivity also uncovered the corresponding insulator to normal-conductor transition in underdoped $La_{2-x}Sr_xCuO_4$ [28]. Noting that at $T = 0$ no thermal fluctuations are left, quantum fluctuations are expected to play an essential role in the zero temperature phase transitions driven by the dopand concentration.

1.1.3 Effective mass anisotropy and spatial dimensionality

Critical properties of a phase transition depend crucially on the spatial dimensionality of the system. Useful information on the dimensionality of cuprate superconductors is obtained from the effective mass anisotropy entering the Ginzburg-Landau Hamiltonian (for a detailed discussion we refer the reader to Sec. 2),

$$\mathcal{H} = \int \mathrm{d}^3R \left(\sum_i \frac{\hbar^2}{2M_i} \left| \frac{\partial}{\partial x_i} \Psi \right|^2 - r|\Psi|^2 + \frac{u}{2}|\Psi|^4 \right), \quad i = x, y, z. \tag{1.1}$$